Observable-dependence of the effective temperature in off-equilibrium diatomic molecular liquids

Andrea Saverio Ninarello,[1] Nicoletta Gnan,[2,a)] and Francesco Sciortino[1,2]
[1]*Dipartimento di Fisica, "Sapienza" Università di Roma, Piazzale A. Moro 2, 00186 Roma, Italy*
[2]*CNR-ISC Uos "Sapienza," Piazzale A. Moro 2, 00186 Roma, Italy*

(Received 8 July 2014; accepted 1 November 2014; published online 20 November 2014)

We discuss the observable-dependence of the effective temperature $T_{\rm eff}$, defined via the fluctuation-dissipation relation, of an out-of-equilibrium system composed by homonuclear dumbbell molecules. $T_{\rm eff}$ is calculated by evaluating the fluctuation and the response for two observables associated, respectively, to translational and to rotational degrees of freedom, following a sudden temperature quench. We repeat our calculations for different dumbbell elongations ζ. At high elongations ($\zeta > 0.4$), we find the same $T_{\rm eff}$ for the two observables. At low elongations ($\zeta \leq 0.4$), only for very deep quenches $T_{\rm eff}$ coincides. The observable-dependence of $T_{\rm eff}$ for low elongations and shallow quenches stresses the importance of a strong coupling between orientational and translational variables for a consistent definition of the effective temperature in glassy systems. © *2014 AIP Publishing LLC*. [http://dx.doi.org/10.1063/1.4901526]

I. INTRODUCTION

Understanding the off-equilibrium state of matter, central in glass science,[1–8] is a challenging task. The difficulty arises from the lack of a thermodynamic approach capable of describing glasses. Indeed, in addition to temperature and pressure, other macroscopic observables are requested to uniquely describe the state of the system. When a liquid is brought off-equilibrium, e.g., by quickly lowering the bath temperature T, dynamic properties depend on the observation time t', i.e., the system ages. Correlation functions retain their two step decay behavior characteristic of supercooled equilibrium states, but show a t' dependence mainly for the α-relaxation process: the structural relaxation time, controlled by the slow modes, increases with the observation time. Aging thus affects the long-time dynamics of particles. The separation of time scales reflects particles vibration around their average position at short times and the diffusional process at long times. As thus, the fast vibrational dynamics equilibrates to T and does not significantly changes with aging.

It has been suggested that the evolution of the correlation function with t' could be interpreted as arising from the slow thermalization of the structural degrees of freedom associated to the α-process. In this respect, one could add to the state variable one or more additional temperatures of the slow modes. While it is clear from experiments based on the Kovacs protocol,[9,10] also reproduced *in silico*,[11,14] that under strong quenching, more than one additional temperature is needed, other protocols are compatible with the idea that one single additional parameter is sufficient to characterize the aging system. In this picture, aging corresponds to the evolution of this additional temperature toward the bath temperature T. In the theoretical framework developed by Cugliandolo and Kurchan,[15,16] the additional temperature reveals its presence in the violation of the fluctuation-dissipation theorem (FDT). In equilibrium, the response of a system to an external weak perturbation is linearly related to a suitable correlation function (and the coefficient of linearity is T). In aging, the fluctuation-dissipation theorem is generalized to account for the presence of an additional temperature, introducing a fluctuation-dissipation (FD) ratio. Given the correlation function $C_{AB}(t, t') = \langle A(t)B(t')\rangle_0$ of two variables $A(t)$ and $B(t)$ in an unperturbed system, and the integrated response $\chi_{A,B}(t, t') = \int_{t'}^{t} \frac{\delta\langle A(t)\rangle_h}{\delta h(s)} ds|_{h\to 0}$ to a perturbation field h applied at a time $t > t'$ (and coupled to the observable $B(t)$), the two functions are related by the expression[4,17]

$$\frac{\partial C_{A,B}(t,t')}{\partial t'} = -\frac{T}{X_{A,B}(t,t')}\frac{\partial \chi_{A,B}(t,t')}{\partial t'}, \tag{1}$$

where

$$X_{A,B}(t,t') = -\frac{1}{T}\frac{\partial \chi_{A,B}(t,t')}{\partial C_{A,B}(t,t')}\bigg|_{\substack{t'=fixed \\ C_{A,B}(t,t')=const}} \tag{2}$$

is the FD ratio. The equilibrium results are recovered when $X_{A,B}(t, t') = 1$ and the FDT is satisfied.

When the system is out of equilibrium the fluctuation and the integrated response are differently related at short and long time-scales. For short time-scales,

$$|X_{A,B}(t,t')| = 1 \quad \text{if } (t-t')/t' \ll 1, \tag{3}$$

i.e., the aging system behaves as if it were in equilibrium, while at long times,

$$|X_{A,B}(t,t')| = \frac{T}{T_{\rm eff}(t,t')} \quad \text{if } (t-t')/t' \gg 1, \tag{4}$$

where $T_{\rm eff}$, named *effective temperature*, has been interpreted as the temperature of the slow degrees of freedom. Thus, while the vibrational dynamics is instantaneously in equilibrium at T after a temperature quench, the slow modes can be thought to be in *quasi*-equilibrium[17,18] at $T_{\rm eff}(t') > T$. The t' dependence clarify that $T_{\rm eff}$ progressively evolves in

a)Electronic mail: nicoletta.gnan@roma1.infn.it

 © 2014 AIP Publishing LLC

time. Hence, the FDR in structural glasses leads naturally to a rigorous definition of $T_{\rm eff}$ that can be evaluated estimating the FD ratio. Evidence of a two-slope FDT in aging systems have been largely provided by numerical simulations of supercooled liquids following temperature or pressure changes.[19–26] For these cases, it has been suggested that $T_{\rm eff}$ coincides with the temperature that a thermometer, weakly coupled to the system, would measure in an aging glass if its internal time-scale is equal to the time-scale of the slow processes in the glass.[7,15] In addition, in some simple molecular glass models, $T_{\rm eff}$ has been shown to coincide with an *internal* temperature independently obtained from an extended thermodynamic framework based on the potential energy landscape (PEL) approach.[23,26,27] Finally, while the assumption of one single additional parameter has been questioned in the past,[9–13] the hypothesis of one single $T_{\rm eff}$ appears to be particularly appropriate in some class of systems.[25,28,29] For these systems, the effective temperature could enter, along with the other equilibrium thermodynamic parameters, in a two-temperatures thermodynamic approach in which a separation of time scales is assumed.[4]

Although the $T_{\rm eff}$ defined from the FDR has been proven to be a valuable concept in several cases, few studies have focused on its observable dependence in structural glasses. Indeed, if $T_{\rm eff}$ can be interpreted as a genuine thermodynamic parameter, it should coincide when measured for different observables on the same time-scale. There is no experimental evidence of the observable independence of $T_{\rm eff}$ in glassy systems and only a few theoretical[16] or numerical investigations.[21,30,31] This issue has also been discussed in the context of granular matter[32–34] or fluids near critical points.[35,36]

In the numerical investigations of Lennard-Jones (LJ) atomic liquids,[30,31] it was found that the FD ratio built from calculating the fluctuations and the responses of density at different wave vectors results in the same $T_{\rm eff}$. However, such result is limited to a single system and all the observables employed in the study are related to translational degrees of freedom. At odd, scarce experimental works have focused on molecular glasses[37–40] and related to the observation of fluctuations and responses of molecules orientation.

In this study, we scrutinize the observable-dependence of $T_{\rm eff}$, by measuring intrinsically different (i.e., translational and rotational) observables. We study the out-of-equilibrium behavior of a system of homonuclear molecules with different elongations, probing both translational and rotational degrees of freedom. We show that various scenarios can occur as a function of the molecules elongation and that distinct observables can be found in distinct aging conditions during the same temperature quench. This results in a partial decoupling of the translational and rotational degrees of freedom and hence in dissimilar FD ratios.

II. MODELS AND METHODS

We perform Metropolis Monte Carlo (MC) simulations of a binary mixture 80 : 20 of $N = 500$ homonuclear dumbbell molecules interacting via a cut-and-shifted LJ potential,[41]

$$V_{\alpha\beta}(r) = 4\varepsilon_{\alpha\beta}\left[\left(\frac{\sigma_{\alpha\beta}}{r}\right)^{12} - \left(\frac{\sigma_{\alpha\beta}}{r}\right)^{6} + A_0 + A_1\frac{r}{\sigma_{\alpha\beta}}\right]. \tag{5}$$

Here, r is the center-to-center distance of two atoms belonging to molecules of type α and β (with $\alpha, \beta \in A, B$). $\sigma_{\alpha\beta}$ and $\epsilon_{\alpha\beta}$ quantify the characteristic size and depth of the interaction potential. The two constants A_0 and A_1 are set to guarantee the continuity of the potential and of its derivative at the cut-off distance $c = 2.5$ (in units of $\sigma_{\alpha\beta}$). From such two constraints one finds that $A_0 = c^{-6}(7 - 13c^{-7})$ and $A_1 = 6c^{-7}(2c^{-6} - 1)$.

Following Ref. 41 we set the interaction parameters to $\sigma_{AA} = 1.0$, $\sigma_{AB} = 0.8$, $\sigma_{BB} = 0.88$, $\epsilon_{AA} = 1.0$, $\epsilon_{AB} = 1.5$, and $\epsilon_{BB} = 0.5$, which correspond to the values first introduced by Kob and Andersen[42,43] for a binary mixture of Lennard-Jones atoms with the aim to prevent the mixture from crystallizing at high densities. In the following, all the parameters will be expressed in reduced units, selecting ϵ_{AA} and σ_{AA} as units of energy and distance. We also set $k_B = 1$. In the case of dumbbell molecules, the total packing fraction $\phi_{tot} = \phi_{AA} + \phi_{BB}$ can be defined as[41]

$$\phi_{\alpha\alpha} = \frac{\pi}{6}\rho_{\alpha\alpha}\sigma_{\alpha\alpha}^3\left(1 + \frac{3}{2}\zeta - \frac{1}{2}\zeta^3\right), \quad 0 \le \zeta \le 1,\ \alpha \in \{A, B\}, \tag{6}$$

where $\rho_{\alpha\alpha} = \frac{N_\alpha}{V}$ is the number density (namely, the number of α dumbbells over the volume), while ζ is the elongation, i.e., the bond length $l_{\alpha\alpha}$ between the centers of the two atoms forming the molecule, expressed in units of $\sigma_{\alpha\alpha}$ (i.e., $\zeta = l_{AA}/\sigma_{AA} = l_{BB}/\sigma_{BB}$). A series of snapshots showing how much the shape of the molecules changes when decreasing ζ are reported in Fig. 1. In our study, we fix the packing fraction to $\phi = 0.708$ in order to compare our equilibrium results with previous Molecular Dynamics (MD) studies at different elongations.[41,44] In such studies, the apparent divergence of the rotational relaxation time τ and the vanishing of the diffusion coefficient D has been estimated according to the theoretical power-law dependence predicted by Mode Coupling Theory (MCT).[44] These values provide a reference for the dynamic arrest temperature. In the following, we define a MC step as N attempts to translate and rotate a randomly selected dumbbell.

Since our work concerns the study of dynamical quantities obtained from a stochastic dynamics (MC), it is legitimate to ask whether the Metropolis algorithm reproduces a long-time dynamical behavior similar to the one observed with Newtonian dynamics[41,44] for the same system. This question has been previously addressed for supercooled binary mixtures of LJ atoms[24] and for models of colloidal particles.[45,46]

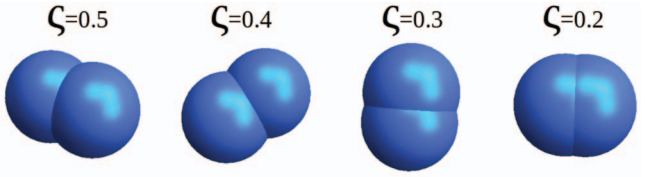

FIG. 1. Snapshots of the dumbbell molecules as a function of the elongation.

These studies have provided evidence that the Metropolis algorithm can give rise to a physically relevant slow dynamics. More precisely, it has been shown that the long-time-decay of the self-intermediate scattering function is identical (with a proper time rescaling) for Newtonian, Brownian,[47] and Monte Carlo simulations.[24] Following a procedure similar to that presented in Ref. 24, we have verified that the long-time relaxation behavior for density and angular correlators in equilibrium LJ dumbbells is equivalent to that evaluated with Newtonian dynamics.[41,44] A detailed discussion for the case of molecules with $\zeta = 0.5$ can be found in the Appendix.

In order to study the FDR, we exploit a zero-field MC algorithm developed and tested previously on atomic structural glasses. This algorithm provides an unbiased measurement of the response function.[31] The method allows us, within the same simulation, the simultaneous measure of both the response and the correlation at different waiting times t' until a fixed time t from the quench, thus reducing the computational load. Following standard works on FDT violation in glasses,[17] we measure $T_{\rm eff}$ by building the FD plot; it consists in reporting $T\chi(t, t')$ versus $C(t, t')$. If the system is characterized by a clear separation of time-scales, as in our case, the resulting parametric curve will display two slopes; the FD ratio $X = T/T_{\rm eff}$ can be immediately visualized being the angular coefficient of the straight line different from $X = 1$. As a rule, we choose to evaluate X via a linear fit of the points in the FD-plot satisfying the relation $(t - t')/t' > 2$.

In this study, we calculate $T_{\rm eff}$ for observables associated to translational and rotational degrees of freedom. For translations, we choose $A_{TRANS}(t) = N^{-1}\sum_j \epsilon_j e^{-i\mathbf{k}\cdot\boldsymbol{r}_j(t)}$ and $B_{TRANS}(t) = 2\sum_j \epsilon_j \cos(\mathbf{k}\cdot\boldsymbol{r}_j(t))$ where the coordinates $\boldsymbol{r}_j(t)$ are the positions of the centers of mass of the molecules at time t and $\epsilon_j = \pm 1$ is a bimodal variable with zero mean which suppresses the cross terms in the correlation and the response functions.[31] Thereby, the correlation function $F_s(\boldsymbol{k}, t, t') \equiv \langle A_{TRANS}(t) B_{TRANS}(t')\rangle_0$ corresponds to the self-intermediate scattering function, where the zero subscript indicates the average over unperturbed trajectories. For rotations we choose $A^{(l)}_{ROT}(t) = \sqrt{\mathcal{N}_l} N^{-1}\sum_i \epsilon_i P_l[\cos(\theta_i(t))]$ and $B^{(l)}_{ROT}(t) = \sqrt{\mathcal{N}_l}\sum_i \epsilon_i P_l[\cos(\theta_i(t))]$, where ϵ_i is a bimodal variable as above, P_l is the Legendre polynomial of order l, and $\theta_i(t) = \hat{e}_i(t)\cdot\hat{x}$ is the projection of the molecular axis on the x-axis. In addition, $\mathcal{N}_l$ is a normalization constant which depends on the order l of the Legendre polynomial and ensures the angular correlation function $C_l(t, t') = \langle A^{(l)}_{ROT}(t) B^{(l)}_{ROT}(t')\rangle_0$ to be 1 when $t = t'$. Specifically, $\mathcal{N}_1 = \frac{1}{3}$ and $\mathcal{N}_2 = \frac{1}{5}$. In the following, we will refer to the FD-plots of the two sets of observables (translation and rotation) as the self-density and the l-orientation FD-plots.

III. RESULTS AND DISCUSSIONS

We perform several temperature quenches by instantaneously lowering the bath temperature from $T = 6$ to $T = 0.4$ for different elongations and we observe the off-equilibrium evolution of the correlators ($F_s(\mathbf{k}, t, t')$ and $C_1(t, t')$) and of the corresponding integrated responses ($\chi_s(\mathbf{k}, t, t')$ and $\chi_1(t, t')$) up to a fixed time t from the quench. This allows us to build the FD-plot from which it is possible to extract $T_{\rm eff}$. A previous study[25] has shown that, in a temperature jump down to a final T, the effective temperature evaluated after a given time t depends weakly on the initial state point as long as the initial T is above the onset temperature of the so-called "landscape-influenced regime"[48] at which the correlation function starts to display a separation of time-scales. This is shown in Fig. 2(c) for two quenches, respectively, $T = 6.0 \to T = 0.4$ and $T = 3.0 \to T = 0.4$, at elongation $\zeta = 0.5$. In the present model, $T = 6.0$ guarantees that we are well above the onset temperature for all elongations. When not specified, we select $|\mathbf{k}| \simeq 8.0$, that roughly corresponds to the first peak of the static structure factor $S(k)$ of the species A. We calculate $T_{\rm eff}$ both in the high elongation region (i.e., $\zeta > 0.4$) and in the low elongation region ($\zeta \leq 0.4$).

A. High elongation region ($\zeta > 0.4$)

We investigate the off-equilibrium dynamics of molecules with elongation $\zeta = 0.45, 0.5, 0.55$. For each elongation, we perform trial quenches and monitor the evolution of the potential energy during aging. We select the smallest investigated waiting time t' when the potential energy starts to show a logarithmic behavior, indicative of a "quasi-stationary" aging regime. We find such time to be $t' = 1800$ MC steps for the three elongations. Successive waiting times are separated one from the other by 1200 MC steps. The total observation time t is set to $t = 29\,400$ MC steps.

We have not been able to investigate the cases with $\zeta > 0.55$. Indeed, for these values rotations are severely frozen; this implies that, when building the $l = 1$-orientation FD-plot, the second slope is not well developed within our observation-time window and we cannot evaluate $T_{\rm eff}$. A measurement of $T_{\rm eff}$ would require prohibitively longer times, inaccessible with our computational facilities.

For $\zeta = 0.45, 0.5, 0.55$, we perform 20 000 independent quenches to ensemble average the correlators and the response functions requested for drawing the FD-plots. Fig. 2(a) clearly shows that, differently from equilibrium, the integrated response (plotted as $1 - T\chi$) evolves in time more slowly than the correlation, both for translational and rotational observables. Figs. 2(b)–2(d) show the three FDT violations. The two-time-scale separation between fast and slow modes in the model system gives rise to FD-plots characterized by two slopes. For both translational and rotational observables, the resulting parametric plots display the same FD ratio $X(t, t')$ and hence the same $T_{\rm eff}$.

Fig. 2(c) ($\zeta = 0.50$) also shows the FD-plot for the self-density evaluated at two other different k vectors. In all cases, the same slope is found, confirming that $T_{\rm eff}$ does not depend on k, in agreement with results for atomic systems.[31,49]

B. Low elongation region ($\zeta \leq 0.4$)

In this region, we investigate molecules with elongations $\zeta = 0.2, 0.3, 0.4$. As for high elongations, we follow the decay of the potential energy during a quench to identify a

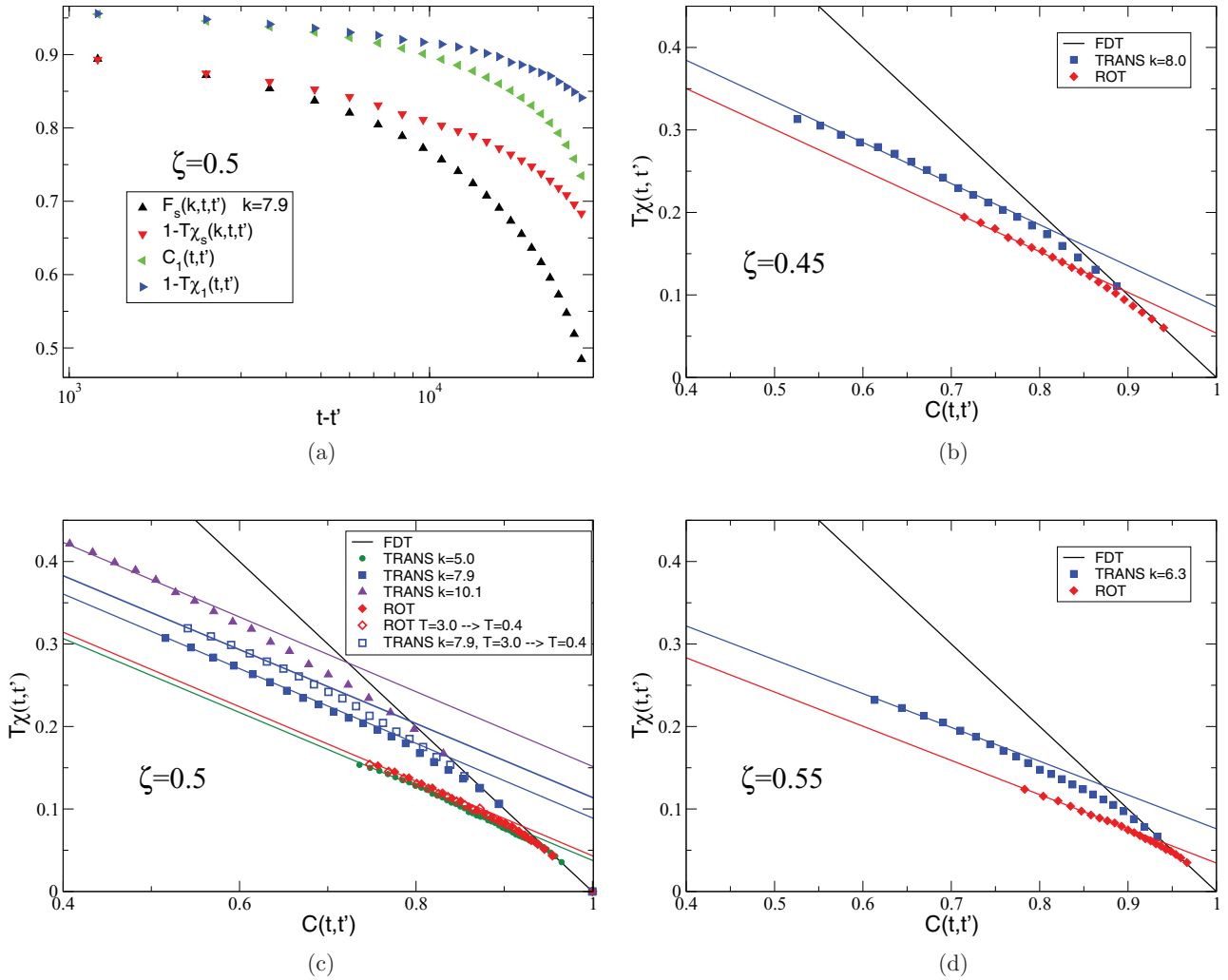

FIG. 2. (a) Correlation and integrated responses as a function of $t - t'$ for the system of LJ dumbbells with elongation $\zeta = 0.5$. Functions are, respectively, $F_s(\mathbf{k}, t, t')$ (black up triangles), $1 - T\chi_s(\mathbf{k}, t, t')$ (red down triangles), $C_1(t, t')$ (green left triangles), and $1 - T\chi_1(t, t')$ (blue right triangles). Data are taken for the quench $T = 6.0 \rightarrow T = 0.4$. (b) Self-density (blue squares) and $l = 1$-orientation (red diamonds) FD-plots for $\zeta = 0.45$. (c) Self-density FD-plots for wave vectors $|\mathbf{k}| = 10.1$ (violet up triangles), $|\mathbf{k}| = 7.9$ (blue squares), and $|\mathbf{k}| = 5.0$ (green circles), together with the $l = 1$-orientation FD-plot (red diamonds) for LJ dumbbells with $\zeta = 0.5$. Open symbols are FD-plots obtained for the quench $T = 3.0 \rightarrow T = 0.4$. (d) Self-density (blue squares) and $l = 1$-orientation (red diamonds) FD-plots for $\zeta = 0.55$.

quasi-equilibrium regime. For the three elongations, we set the first waiting time to $t' = 1800$ MC steps, the same value used for large ζ. As before, successive waiting times are separated by 1200 MC steps and the total observation time is $t = 29\,400$ MC steps. We perform a number of quenches varying between 10 000 and 20 000 for each elongation and we build the self-density and the $l = 1$-orientation FD-plots, finding again the two-slope scenario. However, if we extract T_{eff} from the parametric plots, we find two different effective temperatures for the two FD-plots. The difference between the two T_{eff} increases when decreasing ζ. This is shown in Figs. 3(a) and 3(b), respectively, for $\zeta = 0.4$ and $\zeta = 0.3$. Note that the slope of the FD-plot relative to $l = 1$-orientation is always higher than the slope relative to the density; it follows that the T_{eff} for $l = 1$-orientation is always closer to T than the self-density T_{eff}.

A hint to rationalize the previous results comes from the equilibrium dynamic behavior of the dumbbell molecules in the supercooled regime at different ζ. Previous theoretical and numerical studies[41,44,50] have investigated the dynamic phase diagram of the dumbbells in the $T - \zeta$ plane, showing a strong dependence of the relaxation dynamics on the elongation of the molecules. For instance, numerical simulations[44] have shown that iso-diffusivity lines are non-monotonic functions of the elongation. The behavior of the rotations is also intriguing: depending on the degree l of the Legendre polynomial employed to build $C_l(t)$, the observed dynamics and the isochronal iso-τ_l curves (where τ_l is the relaxation time of $C_l(t)$) can be different (inset of Fig. 3(b)). Specifically, for even-l correlators, e.g., $C_{l=2}(t)$, the iso-τ_2 curve closely follows the iso-diffusivity line in the $T - \zeta$ plane. Contrary, the iso-τ_1 line of $C_1(t)$ is coupled to the iso-D and to the iso-τ_2 curves only at high ζ, while the coupling is lost for lower ζ. In this decoupled region, $C_1(t)$ relaxes to zero significantly faster than $C_2(t)$. This peculiar behavior has been explained in terms of hopping processes occurring in the low-elongation region. Indeed, it has been observed that low-elongation molecules perform rotational flips

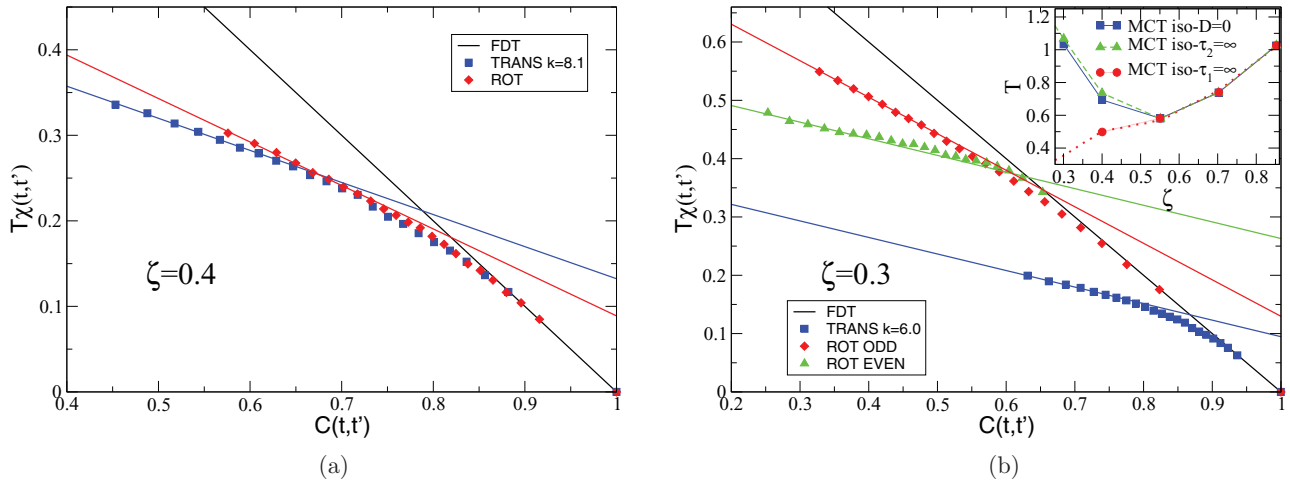

FIG. 3. Self-density (blue squares) and $l = 1$-orientation (red diamonds) FD-plots for dumbbells with elongation (a) $\zeta = 0.4$ and (b) $\zeta = 0.3$, for the quench $T = 6.0 \rightarrow T = 0.4$. Green squares in (b) is the $l = 2$-orientation FD-plot, associated to even rotations of molecules. Inset: MCT arrested lines, i.e., the loci of points predicted by Mode Coupling Theory at which the diffusion coefficient is $D = 0$ (blue-squares), the decay time of $C_1(t)$ is $\tau_1 = \infty$ (red circles) and that of $C_2(t)$ (dashed dotted line) is $\tau_2 = \infty$ (green triangles) in the $T - \zeta$ plane. Data from Ref. 44.

of 180° which change sign to P_1 (and to all odd Legendre replace polynomial with polynomials), providing the dominant contribution to the decorrelation of $C_1(t)$. According to Mode-Coupling Theory for monodisperse dumbbells,[50] a critical value for the molecules elongation $\zeta_c = 0.345$ marks the crossover between the strong-to-weak hindrance scenario described above. Simulations also suggest a value close to ζ_c for the present binary mixture of dumbbells. These equilibrium results provide two important pieces of evidence: (i) that there is a cross-over between small and large ζ values, associated to a decoupling of rotation and translation for odd l, (ii) that the decay of the odd l correlation functions for small ζ proceed much faster than the decay of the other correlators.

Based on these findings we investigate the off-equilibrium behavior of the $l = 2$ orientation $C_2(t, t')$ and its integrated response $\chi_2(t, t')$ when $\zeta = 0.3$. Figure 3(b) shows the resulting $l = 2$-orientation FD-plot: we find that, as for the equilibrium case, the aging behavior of observables associated to translational and $l = 2$-rotational degrees of freedom are strongly coupled. Differently from what found for $l = 1$, the two FD-plots display now the same T_{eff}.

As a last piece of evidence, we investigate the sensitivity of the previous results to the quench depth. Figure 4 shows the result for $\zeta = 0.3$ following a quench from $T = 6.0$ to $T = 0.2$. At this low T, we expect (based on extrapolation of the T-dependence of the equilibrium rotational and translational characteristic times) that also the $l = 1$ correlator is unable to thermalize. Indeed, we find that when T is low enough, the odd-rotations are frozen and hence coupled to the density, being described by the same T_{eff}.

Finally, to gain insight into the off-equilibrium dynamics of molecular rotations, we study the t dependence of T_{eff} by comparing the correlators and the response functions for two different waiting time t' for the quench $T = 6.0 \rightarrow T = 0.4$. Figure 5 shows the self-density and the $l = 1$-orientation FD-plots for the observation times $t_1 = 29\,400$ and $t_2 = 79\,200$

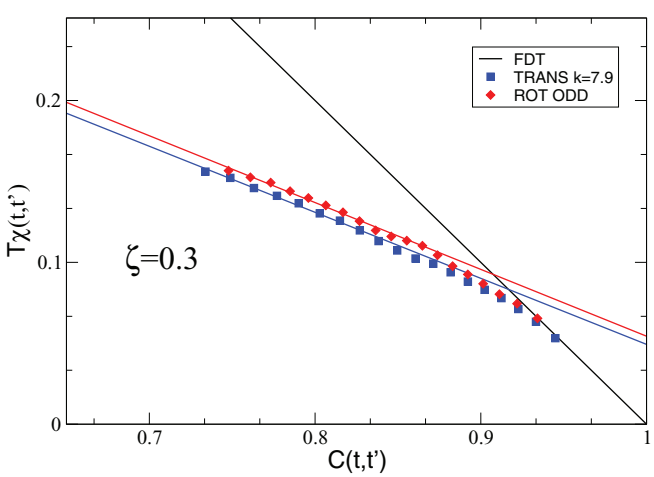

FIG. 4. Self-density and $l = 1$-orientation FD-plots for the system of dumbbells with $\zeta = 0.3$ for the quench $T = 6.0 \rightarrow T = 0.2$.

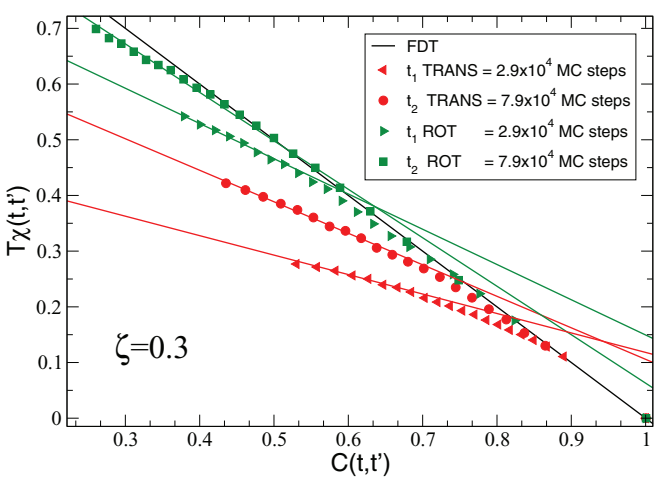

FIG. 5. Self-density and $l = 1$-orientation FD-plots for the system of dumbbells with $\zeta = 0.3$ for a quench from $T = 6$ to $T = 0.4$. Data plotted as (red) left and (green) right triangles are measured for a total time of $t = 29\,400$ MC steps, while for (red) circles and (green) squares the total observation time is set to $t_2 = 79\,200$ MC steps.

MC steps. We note that for both translational and rotational degrees of freedom the slope of the FD-plot changes with t', in agreement with previous observations for atomic systems,[23] highlighting the presence of a slow aging process. We also note that while the $T_{\rm eff}$ of the self-density always remains very different from T, the $l = 1$-orientation appears to have almost completely thermalized at the largest t' value.

IV. CONCLUSIONS

The idea of considering the $T_{\rm eff}$ entering in the FD-ratio as a thermodynamic parameter that accounts for the aging of the slow modes in structural glasses has been widely discussed in many different frameworks. One of the requests for being a robust thermodynamic variable is its independence from the (slow) observable measured.[18] For this purpose, we investigated the off-equilibrium dynamics of a van der Waals liquid composed of a binary mixture of dumbbell molecules, by studying the fluctuations and the responses of observables associated both to translational and rotational motions. Thus, we have been able to carry on a more complete study with respect to the case of the atomic Lennard-Jones, where only the wave-vector dependence of the density correlator[24,51] was investigated. In this article, we have reported the first computational measurements of the FDR for rotational degrees of freedom in a molecular liquid. We note in passing that previous experimental studies of the FDT violation were built on the observation of rotational dynamics, based on depolarized light-scattering or dielectric spectroscopy.[37–40] The evaluation of $T_{\rm eff}$ at different elongations highlighted a rich and unexpected scenario. We focused on the off-equilibrium dynamics of density and orientation fluctuations of the molecules and we observed that, for high elongations, rotational and translational degrees of freedom are characterized by the same $T_{\rm eff}$. Such situation is partially lost at lower elongations. For small elongations and shallow quenches, odd rotational degrees of freedom are characterized by different FD-plots as compared to the translational ones, and the $T_{\rm eff}$ of the rotational degrees of freedom approaches the bath temperature. For small elongations and deep quenches, the effective temperatures of the translational and rotational observables couple again.

These findings bear a resemblance with the ζ dependence of the equilibrium rotational and translational behavior. At small ζ, molecules undergo rotations of 180° which allow $C_1(t)$ (but not $C_2(t)$) to relax fast,[44] decoupling translations and rotations. As a consequence, at equilibrium, $C_1(t)$ does not show a separation of time-scales at temperatures where $F_s(\mathbf{k}, t)$ and $C_2(t)$ are instead characterized by the typical two-step decay. Indeed, in the limit of zero elongation, rotations are completely free and decoupled from translations. Our results suggests that only at very deep temperatures, odd-rotational dynamics couples again to translations. Indeed, only for deep quenches, the $l = 1$-orientation and the self-density FD-plots display the same $T_{\rm eff}$. The $l = 2$-orientation instead is always coupled with density. We find that for shallow quenches, the violation of the FDT for the $l = 1$-orientation is a transient effect. Hence, in a hypothetical experiment on molecular liquids with low elongation, the measurement of the fluctuations and of the responses of observables coupled with degrees of freedom not sensitive to the hopping processes will lead to a resulting $T_{\rm eff}$ which reflects the same aging behavior of the translational degrees of freedom. Differently, $l = 1$ observables may or may not couple to translational degrees of freedom. The possibility thus exists that the effective temperature of the odd angular correlator might differ from the one of the translational degrees of freedom. To establish a connection with possible experiments we note that our dumbbell model, at least for intermediate elongations, could be a realistic model for toluene, a molecule composed by a phenyl group and a methyl group that can be approximated as spheres. The two groups have different sizes and hence a better representation of toluene would be an asymmetric dumbbell. Still, assuming the symmetric dumbbell model, all the quenches done in our study, would be compatible with temperature jumps from ambient T to around 40 K. Keeping the correspondence with toluene, we can also extract information on the timescales at which we observe the violation of the FDT. In fact, we can use the mapping between Monte Carlo and molecular dynamics time steps described in the Appendix, to obtain an estimation of the observation time in our simulations. Then, using the parameters for mass, size, and energy scale for the phenyl group (following Ref. 52), we find that our observation time (∼30 000 MC steps) roughly corresponds to a few nanoseconds, a timescale that can be accessed, for example, via neutron scattering experiments or broadband dielectric spectroscopy.

Finally, we want to stress that recent theoretical arguments[34] provided evidence that, in off-equilibrium stationary states, the observable independence of $T_{\rm eff}$ is related to the uniformity of the phase space distribution. It would be interesting to understand in future studies how our results connect with this appealing theoretical result.

ACKNOWLEDGMENTS

N.G. acknowledges the support from MIUR-FIRB ANISOFT (RBFR125H0M). We thank A. Puglisi, A. Sarracino, and A. Crisanti for discussions.

APPENDIX: COMPARISON WITH NEWTONIAN DYNAMICS

In our simulations, a Monte Carlo step is defined as N attempts to translate and rotate a molecule chosen randomly. Translations are uniformly extracted in the interval $[-\delta r_{MAX}, \delta r_{MAX}]$ while rotations are performed around a randomly chosen axis with an angle uniformly distributed within the interval $[-\delta\alpha_{MAX}, \delta\alpha_{MAX}]$. The attempt to move a molecule is rejected or accepted according to the Metropolis rule.[53] Hence, the acceptance rate, and consequently the dynamics, depends on the balance between the two parameters δr_{MAX} and $\delta\alpha_{MAX}$. Since the acceptance rate has not to be neither too small nor too high (i.e., should range between 30% and 60% of the total attempts) to provide a long-time dynamics consistent with the Newtonian one, we set the acceptance rate in our simulation to 45%. Given this, there are a number of combinations for δr_{MAX} and $\delta\alpha_{MAX}$ that satisfy the condition on the acceptance rate. We then perform a number of simulations in the

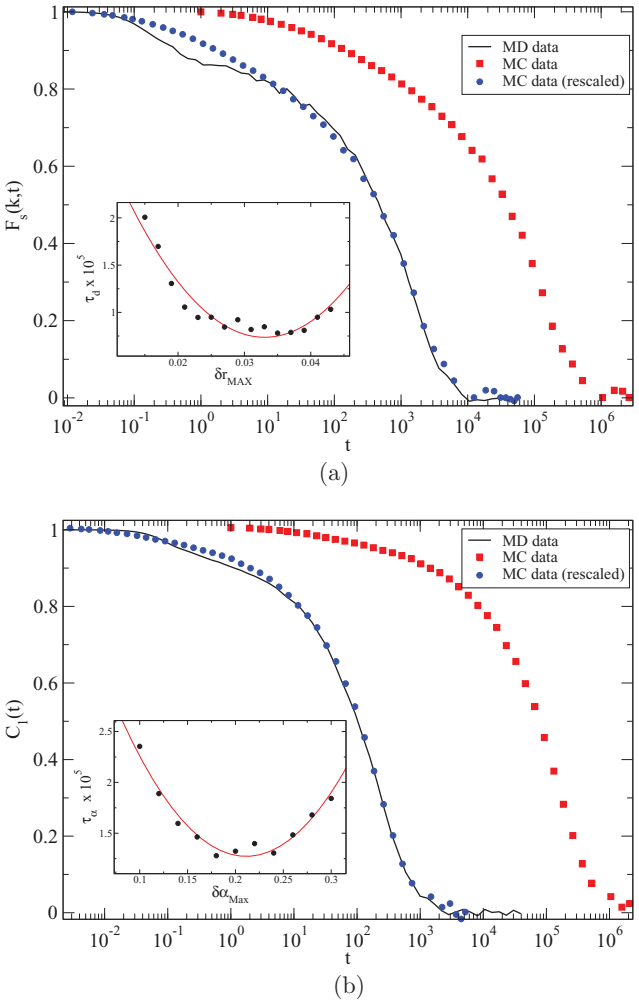

FIG. 6. (a) Self-intermediate scattering function $F_s(\mathbf{k}, t)$ and (b) autocorrelation function $C_1(t)$ of the first Legendre polynomial for dumbbell molecules with elongation $\zeta = 0.5$ at the state point $T = 0.75$, $\phi = 0.708$. Symbols are results from MC dynamics and solid lines from Newtonian dynamics (data taken from Ref. 41). Insets: evolution of the relaxation times (a) for $F_s(k, t)$ as a function of δr_{MAX}, (b) for $C_1(t)$ as a function of $\delta\alpha_{MAX}$. The minimum values of δr_{MAX} and $\delta\alpha_{MAX}$ used in MC simulations provide a relaxation behavior of functions in (a) and (b), compatible with the results obtained in molecular dynamic simulations.

canonical ensemble where the two parameters are varied and we observe the relaxation of density and angular correlation functions. We report here the results for the intermediate state point $T = 0.75$, $\phi = 0.708$ when the elongation of the dumbbell is set to $\zeta = 0.5$, but the procedure to follow is the same at all the elongations.

We extract from simulations the relaxation times of the self-intermediate scattering function τ_d and of the angular correlator τ_α, defined as the value at which the correlation functions decay at $1/e$. The relaxation times (in unit of MC step) τ_d and τ_α as a function of δr_{MAX} and $\delta\alpha_{MAX}$ are shown in the insets of Figs. 6(a) and 6(b), respectively. Due to their non-monotonic behavior we are able to extrapolate through a parabolic fit the value at which τ_d and τ_α are minimized, finding $\delta r_{MAX} = 0.025$ and $\delta\alpha_{MAX} = 0.20$. Figures 6(a) and 6(b) show that for such values, the long-time decay of the angular correlation function and of the self-intermediate scattering function can be superimposed on top of the corresponding correlators obtained from Newtonian dynamics, after having scaled the x-axis of the MC curves by an arbitrary factor.

[1] W. Goetze, *Complex Dynamics of Glass-forming Liquids: A Mode Coupling Theory*, 1st ed. (Oxford University Press, Oxford, 2009).
[2] K. Binder and W. Kob, *Glassy Materials and Disordered Solids: An Introduction to their Statistical Mechanics*, 1st ed. (World Scientific, Singapore, 2005).
[3] P. G. Wolynes and V. Lubchenko, *Structural Glasses and Supercooled Liquids*, 1st ed. (Wiley, Hoboken, NJ, 2012).
[4] L. Leuzzi, J. Non-Cryst. Solids **355**, 686 (2009).
[5] L. Berthier and G. Biroli, Rev. Mod. Phys. **83**, 587 (2011).
[6] G. Biroli and J. P. Garrahan, J. Chem. Phys. **138**, 12A301 (2013).
[7] J. Kurchan, Nature (London) **433**, 222 (2005).
[8] M. D. Ediger, C. A. Angell, and S. R. Nagel, J. Chem. Phys. **100**, 13200 (1996).
[9] A. J. Kovacs, Fortschr. Hochpolym.-Forsch. **3**, 394 (1963).
[10] C. A. Angell *et al.*, J. Appl. Phys. **88**, 3113 (2000).
[11] S. Mossa and F. Sciortino, Phys. Rev. Lett. **92**, 045504 (2004).
[12] J. S. Langer, Phys. Rev. E **70**, 041502 (2004).
[13] E. Bouchbinder and J. S. Langer, Phys. Rev. E **80**, 031132 (2009).
[14] I. Saika-Voivod and F. Sciortino, Phys. Rev. E **70**, 041202 (2004).
[15] L. F. Cugliandolo, J. Kurchan, and L. Peliti, Phys. Rev. E **55**, 3898 (1997).
[16] L. Cugliandolo and J. Kurchan, J. Phys. Soc. Jpn., Suppl. A **69**, 247 (2000).
[17] A. Crisanti and F. Ritort, J. Phys. A **36**, R181 (2003).
[18] L. Cugliandolo, J. Phys. A **44**, 4830001 (2011).
[19] G. Parisi, Phys. Rev. Lett. **79**, 3660 (1997).
[20] J.-L. Barrat and W. Kob, Europhys. Lett. **46**, 637 (1999).
[21] W. Kob and J. Barrat, Eur. Phys. J. B **13**, 319 (2000).
[22] R. D. Leonardo, L. Angelani, G. Parisi, and G. Ruocco, Phys. Rev. Lett. **84**, 6054 (2000).
[23] F. Sciortino and P. Tartaglia, Phys. Rev. Lett. **86**, 107 (2001).
[24] L. Berthier and W. Kob, J. Phys.: Condens. Matter **19**, 205130 (2007).
[25] N. Gnan, C. Maggi, T. Schroeder, and J. Dyre, Phys. Rev. Lett. **104**, 125902 (2010).
[26] N. Gnan, C. Maggi, G. Parisi, and F. Sciortino, Phys. Rev. Lett. **110**, 035701 (2013).
[27] F. Sciortino, J. Stat. Mech. Theor. Exp. **2005**, P05015.
[28] U. R. Pedersen, T. Christensen, T. B. Schroeder, and J. Dyre, Phys. Rev. E **77**, 011201 (2008).
[29] N. P. Bayley *et al.*, J. Chem. Phys. **129**, 184507 (2008).
[30] L. Berthier and J.-L. Barrat, J. Chem. Phys. **116**, 6228 (2004).
[31] L. Berthier, Phys. Rev. Lett. **98**, 220601 (2007).
[32] P. Viot and J. Talbot, Phys. Rev. E **69**, 051106 (2004).
[33] D. Villamaina, A. Baldassarri, A. Puglisi, and A. Vulpiani, J. Stat. Mech. Theor. Exp. **2009**, P07024.
[34] K. Martens, E. Bertin, and M. Droz, Phys. Rev. Lett. **3**, 260602 (2009)
[35] P. Calabrese and A. Gambassi, J. Stat. Mech. Theor. Exp. **2005**, P07013.
[36] S. Joubaud, B. Percier, A. Petrosyan, and S. Ciliberto, Phys. Rev. Lett. **102**, 130601 (2009).
[37] T. S. Grigera and N. E. Israeloff, Phys. Rev. Lett. **83**, 5038 (1999).
[38] L. Buisson and S. Ciliberto, Physica D **204**, 1 (2005).
[39] J. Schindele, A. Reiser, and C. Enss, Phys. Rev. Lett. **107**, 095701 (2011).
[40] H. Oukris and N. E. Israeloff, Nat. Phys. **6**, 135 (2010).
[41] S.-H. Chong, A. J. Moreno, F. Sciortino, and W. Kob, Phys. Rev. Lett. **94**, 215701 (2005).
[42] H. C. Andersen and W. Kob, Phys. Rev. E **51**, 4626 (1995).
[43] H. C. Andersen and W. Kob, Phys. Rev. E **52**, 4134 (1995).
[44] A. J. Moreno, S.-H. Chong, W. Kob, and F. Sciortino, J. Chem. Phys. **123**, 204505 (2005).
[45] E. Sanz and D. Marenduzzo, J. Chem. Phys. **132**, 194102 (2010).
[46] F. Romano, C. De Michele, D. Marenduzzo, and E. Sanz, J. Chem. Phys. **135**, 124106 (2011).
[47] T. Gleim *et al.*, Phys. Rev. Lett. **81**, 4404 (1998).
[48] S. Sastry, P. G. Debenedetti, and F. H. Stillinger, Nature (London) **393**, 554 (1998).
[49] J.-L. Barrat and W. Kob, J. Phys. Condens. Matter **11**, A247 (1999).
[50] S.-H. Chong and W. Götze, Phys. Rev. E **65**, 041503 (2002).
[51] L. Berthier, Phys. Rev. E **69**, 020201 (2004).
[52] T. B. Schrøder, U. R. Pedersen, N. P. Bailey, S. Toxvaerd, and J. C. Dyre, Phys. Rev. E **80**, 041502 (2009).
[53] N. Metropolis *et al.*, J. Chem. Phys. **21**, 1087 (1953).